

Journal Pre-proof

Multicomponent and 1,3-dipolar cycloaddition synthesis of triazole- and isoxazole-acridinedione/xanthenedione heterocyclic hybrids: Cytotoxic effects on human cancer cells

Abdelkader Naouri, Amar Djemoui, Mouhamad Ridha Ouahrani, Mokhtar Boualem Lahrech, Najet Lemouari, Djenisa H.A. Rocha, Hélio Albuquerque, Ricardo F. Mendes, Filipe A.Almeida Paz, Luisa A. Helguero, Khaldoun Bachari, Oualid Talhi, Artur M.S. Silva

PII: S0022-2860(20)30650-5

DOI: <https://doi.org/10.1016/j.molstruc.2020.128325>

Reference: MOLSTR 128325

To appear in: *Journal of Molecular Structure*

Received Date: 11 January 2020

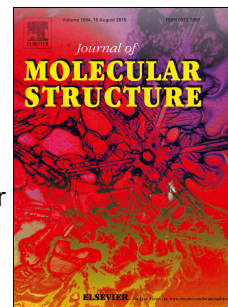
Revised Date: 21 April 2020

Accepted Date: 23 April 2020

Please cite this article as: A. Naouri, A. Djemoui, M.R. Ouahrani, M.B. Lahrech, N. Lemouari, D.H.A. Rocha, Hé. Albuquerque, R.F. Mendes, F.A.A. Paz, L.A. Helguero, K. Bachari, O. Talhi, A.M.S. Silva, Multicomponent and 1,3-dipolar cycloaddition synthesis of triazole- and isoxazole-acridinedione/xanthenedione heterocyclic hybrids: Cytotoxic effects on human cancer cells, *Journal of Molecular Structure* (2020), doi: <https://doi.org/10.1016/j.molstruc.2020.128325>.

This is a PDF file of an article that has undergone enhancements after acceptance, such as the addition of a cover page and metadata, and formatting for readability, but it is not yet the definitive version of record. This version will undergo additional copyediting, typesetting and review before it is published in its final form, but we are providing this version to give early visibility of the article. Please note that, during the production process, errors may be discovered which could affect the content, and all legal disclaimers that apply to the journal pertain.

© 2020 Published by Elsevier B.V.



Credit author statement:

Naouri Abdelkader conceptualized the work and wrote the original draft preparation.

Amar Djemoui performed the synthetic experimental work and co-wrote the manuscript.

Ouahrani Mohammad Ridha and **Lahrech Moukhtar Boualem** participated in the synthetic experimental work (purification, isolation and recrystallisation).

Najet Lemouari and **Hélio Albuquerque** performed 2D-NMR analysis and interpretations

Djenisa H. A. Rocha and **Luisa A. Helguero** performed the anticancer biological assays

Ricardo F. Mendes and **Filipe A. Almeida Paz** were responsible for all X-ray diffraction work.

Khaldoun Bachari, **Oualid Talhi** and **Artur M. S. Silva** co-conceptualized the work and co-wrote the manuscript.

Multicomponent and 1,3-dipolar cycloaddition synthesis of triazole- and isoxazole-acridinedione/xanthenedione heterocyclic hybrids: cytotoxic effects on human cancer cells

Abdelkader Naouri,^{a,b,c,*} Amar Djemoui,^{a,b} Mouhamad Ridha Ouahrani,^d Mokhtar Boualem Lahrech,^b Najet Lemouari,^c Djenisa H. A. Rocha,^{e,f,g} Hélio Albuquerque,^c Ricardo F. Mendes,^f Filipe A. Almeida Paz,^f Luisa A. Helguero,^g Khaldoun Bachari,^c Oualid Talhi,^{c,e,*} and Artur M. S. Silva^{e,*}

^aDepartment of Chemistry, Faculty of Exact Sciences and Informatics ZIANE Achour University, Djelfa, Algeria. abdelkader.naouri@crapc.dz

^bLaboratory of Organic Chemistry and Natural Substance, Faculty of Exact Sciences and informatics, ZIANE Achour University, Djelfa, Algeria.

^cCentre de Recherche Scientifique et Technique en Analyses Physico-Chimiques, CRAPC, BP384, Bou-Ismaïl, 42004, Tipaza, Algeria. oualid.talhi@crapc.dz

^dDepartment of Chemistry, Faculty of Exact Sciences, Echahid Hamma Lakhdar University of El Oued, Eloued, Algeria.

^eQOPNA and LAQV-REQUIMTE, Department of Chemistry, University of Aveiro, 3810-193, Aveiro, Portugal. oualid.talhi@ua.pt, artur.silva@ua.pt

^fCICECO-Aveiro Institute of Material, University of Aveiro, 3810-193, Aveiro, Portugal.

^gInstitute of Biomedicine (iBiMED), Department of Medical Sciences, University of Aveiro, 3810-193, Aveiro, Portugal.

ABSTRACT

A new series of diverse 1,2,3-triazole-acridinedione/xanthenedione and 1,2-isoxazole-acridinedione/xanthenedione heterocyclic hybrids have been synthesized via 1,3-dipolar coupling reaction of *N/O*-substituted-acridinedione-alkyne or *O*-substituted-xanthenedione-alkyne substrates with various aromatic azides or oximes. In all cases, the cycloaddition is totally regioselective. The chemical structures of the synthesized compounds are determined using 2D NMR and are further confirmed by single-crystal X-ray diffraction analysis. Preliminary in vitro cytotoxic assays on two human breast cancer cell lines (MDA-MB-231, T47-D) and one prostate cancer cell line (PC3) are performed on some selected compounds. The most active *O*-1,2,3-triazole-xanthenedione hybrid displays the best cytotoxicity effects with $IC_{50} \leq 20 \mu\text{M}$ in breast cancer and $IC_{50} = 10 \mu\text{M}$ in prostate cancer cell lines.

Keywords: Click chemistry, Triazole, Isoxazole, Acridinedione, Xanthenedione, Anticancer

* Corresponding author. e-mail: abdelkader.naouri@crapc.dz, oualid.talhi@ua.pt, artur.silva@ua.pt

The modern trend in organic chemistry is actually the synthesis of combined organic molecules, especially heterocycles, as potentially useful structural motifs for drugs and pharmaceutical industry. Due to the growing need for potent bioactive compounds for public health, researchers are mostly oriented towards developing newer, more effective and less toxic molecules showing specific and selective biological mode of actions and improved properties. In this regard, a number of new compounds have been designed bearing various biological activities by the combination of at least two or more pharmacophores in "one chemical structure". The use of green chemistry towards the elaboration of bioorganic-nanomaterial hybrids have recently evidenced impactful biomedical applications.¹ Incorporating five- and six-membered nitrogen and oxygen containing heterocycles to generate the so-called "hybrid molecule" has been proved to be effective in terms of enhanced activity, when compared to that of individual pharmacophores.¹

Triazoles and isoxazoles are important classes of nitrogen and oxygen containing five-membered heterocycles, being useful in drug design and known as privileged structures.² Triazoles are mostly applied in medicinal,³ pharmaceutical,⁴ biological⁵ and material sciences.⁶ This heterocyclic motif is found as a fingerprint of some known drugs such as fluconazole⁷ (Figure 1). Triazoles and isoxazoles have a wide range of biological properties such as anticancer,⁸ anti-HIV,⁹ antibacterial,¹⁰ antimalarial¹¹ and anti-tubercular¹² activities. Particularly, triazoles are stable to hydrolysis, oxidation and relatively resistant to metabolic degradation.¹³ On the other side, isoxazoles are found as the basic structure of remarkable drugs, for example, the antibiotic sulfamethoxazole¹⁴ (Figure 1).

A variety of synthetic routes have been reported for the synthesis of triazoles and isoxazoles, being one of the most popular the [3+2] cycloaddition of alkynes with azides or nitrile oxides, respectively.¹⁵ In parallel, we found that the multicomponent reaction (MCR) approach has been widely used for the production of complex and highly diverse nitrogen and oxygen containing six-membered heterocycles such as acridine and xanthene. MCRs are experimentally performed in shorter time and in a single step allowing excellent yields and highly pure compounds. By using easily accessible starting materials, outstanding acridine templates containing 1,4-dihydropyridines (1,4-DHPs) and xanthenediones with a pyrane ring have been accessed via MCRs without the isolation of reaction intermediates.¹⁵ These structures have also shown a wide range of pharmacological and biological activities.¹⁶ DHPs were firstly developed as cardiovascular agents¹⁷, but they have also found applications for other medicinal treatments, for instance, nifedipine which is employed in the treatment of migraine, hypertrophic cardiomyopathy and Raynaud's phenomenon¹⁸ (Figure 1). Among the various subclasses of pyrans, 9-arylxanthenes are active oxygenated heterocycles, which are important drug intermediates. They are known as, anti-inflammatory,¹⁹ antiviral,²⁰ antibacterial²¹ agents and thoroughly used in photodynamic therapy to destroy tumor cells.²² Xanthene derivatives are widely utilized in laser technology because of their interesting spectroscopic properties,²³ in fluorescent materials for the visualization of biomolecules²⁴ and especially as dyes like the popular rhodamine 6G²⁵ (Figure 1).

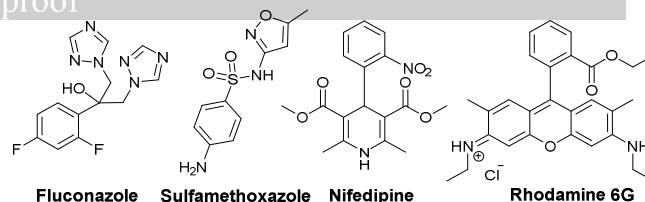


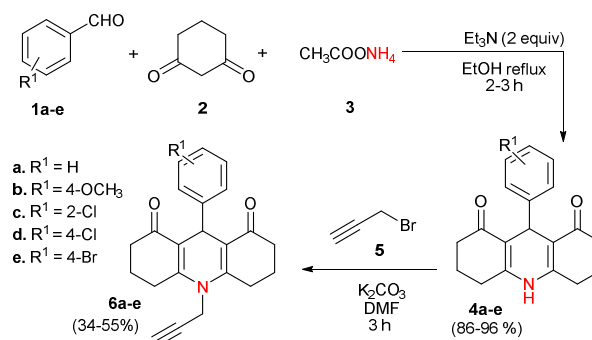
Figure 1. Examples of interesting structures bearing of triazole, isoxazole, acridine and xanthene motifs.

In light of the biological and technological importance of the aforementioned nitrogen and oxygen containing five- and six-membered heterocycles, it is very interesting to develop new structures incorporating acridine and xanthene with 1,2,3-triazole and 1,2-isoxazole motifs in hybrid molecules. In this context, we describe efficient syntheses of a novel series of 1,4-disubstituted 1,2,3-triazoles and 3,5-disubstituted 1,2-isoxazoles by regioselective reaction of arylazides and aryloximes with the N-/O-acridinedione and O-xanthenedione derived terminal alkynes via click chemistry. Preliminary anticancer screening of these hybrid heterocycles performed on two human breast cancer (MDA-MB-231, T47-D) and one prostate cancer cell lines (PC3) shows promising effects

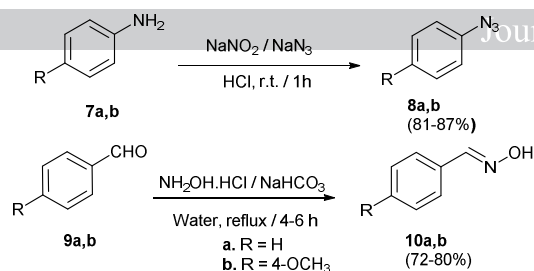
2. Results and discussion

2.1. Chemistry and spectral analysis

We first describe the synthesis of *N*-1,2,3-triazole-dioxodecahydroacridine **11a-e** and *N*-1,2-isoxazole-dioxodecahydroacridine **12a-e** heterocyclic hybrids via Click reaction. The procedure begins by the preparation of 1,8-dioxodecahydroacridine derivatives via a one-pot three-component condensation of aromatic aldehydes **1a-e**, 1,3-cyclohexanedione **2** and ammonium acetate **3** in ethanol catalyzed by triethylamine (TEA) to give the desired intermediates **4a-e** in excellent yields (86-96%) (Scheme 1).²⁶ Then the *N*-alkylation of 1,8-dioxodecahydroacridines **4a-e** with propargyl bromide **5** in presence of K_2CO_3 as a base and DMF as solvent at room temperature were carried out. The reaction normally takes place in 3 hours to afford the corresponding *N*-propargyl-substituted 1,8-dioxodecahydroacridines **6a-e** obtained in moderate yields (34-55%, Scheme 1). In the following step, arylazides **8a,b** were prepared by reacting aniline derivatives **7a,b** with sodium nitrite and sodium azide in acidic medium at room temperature. The reaction of aldehydes **9a,b** with hydroxylamine hydrochloride in refluxing water under basic ($NaHCO_3$) conditions provides the corresponding aryloximes **10a,b** (Scheme 2).



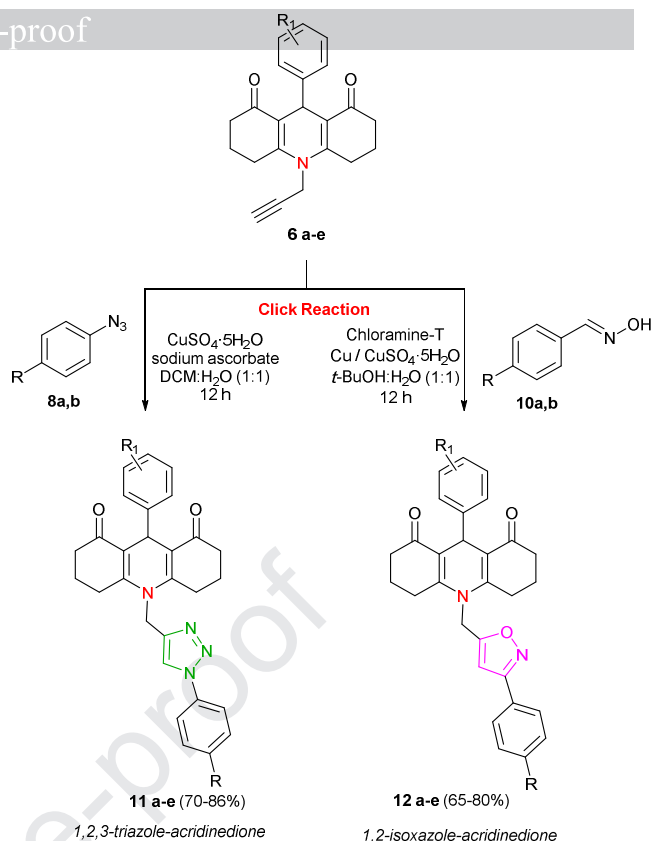
Scheme 1. Synthesis of 1,8-dioxodecahydroacridines **4a-e** and their *N*-propargylated derivatives **6a-e**.



Scheme 2. Preparation of arylazides **8a,b** and aryloximes **10a,b**.

The last step settles in a simple 1,3-dipolar cycloaddition reactions between *N*-propargyl-substituted-1,8-dioxodecahydroacridines **6a-d** with aromatic azides **8a,b**, in the presence of CuSO₄·5H₂O/ascorbic acid as catalyst in a 2:1 mixture of dichloromethane:H₂O at room temperature for 12 h to produce 1,2,3-triazole-dioxodecahydroacridine hybrids **11a-e** in good to excellent yield (70-86%) (Scheme 3). On the other hand, subjecting *N*-propargyl-substituted 1,8-dioxodecahydroacridines **6a-d** to [3+2] cycloaddition reaction with various aryloximes **10a,b** in the presence of chloramine-T, CuSO₄ and Cu powder furnished the desired 1,2-isoxazole-dioxodecahydroacridine hybrids **12a-e** (65-80%) (Scheme 3).

The combination of ¹H and ¹³C NMR spectroscopy allows a clear determination of the regioselective formation of a unique 1,4-disubstituted 1,2,3-triazole ring in the 1,2,3-triazole-*N*-acridinedione and 1,2-isoxazole-*N*-acridinedione hybrids. The characteristic signal of the triazolic H-5'' of compound **11a** appears as a singlet at δ_H 8.75 ppm, while that of isoxazole **12a** showed the singlet H-4'' around δ_H 6.89 ppm. Aliphatic signals at δ_H 5.18, 5.29 ppm are assigned to the methylene H-1' linking the heterocyclic moieties (triazole or isoxazole) to the acridine bulk. ¹³C NMR of **11a** displayed the triazole skeleton with C-5'' at δ_C 121.8 and the quaternary C-4'' at δ_C 145.2 ppm based on its HMBC correlations established with H-1' and H-5'' (Figure 2). For the isoxazole **12a**, one protonated carbon C-4'' (δ_C 101.0 ppm) and two different quaternary carbons C-3'' and C-5'' are distinguished, being respectively attributed to δ_C 162.10, 169.4 ppm and confirmed through HMBC correlations entertained between C-3''/H-4'' and C-5''/H-1'/H-4'' (Figure 2). Other important HMBC cross-peak correlations have been studied, which greatly help us to establish the symmetrical structure of acridine, especially those observed between H-9' with its neighbouring quaternary carbons C8a/9a (δ_C 115.2-116.0 ppm), C-4a/10a (δ_C 153.9-154.2 ppm) and the carbonyl C-1 (δ_C 195.7-195.8 ppm) of both hybrid structures **11a** and **12a** (Figure 2, ESI for NMR spectra).



Scheme 3. Synthesis of *N*-1,2,3-triazole-dioxodecahydroacridines **11a-e** and *N*-1,2-isoxazole-dioxodecahydroacridines **12a-e** via click reaction.

Good quality single-crystals have only been successfully obtained for the isoxazole-acridine template **12a**, being isolated from a 1:1 mixture of hexane:dichloromethane by slow evaporation at *ca.* 6 °C. The crystal structure was determined in the centrosymmetric triclinic *P* $\bar{1}$ space group. The asymmetric unit is composed of a whole molecular unit of **12a** plus partially-occupied water and dichloromethane solvent molecules (Figure 3). Remarkably, though the molecule is rich in atoms capable of being engaged in strong hydrogen bonds and acceptors, there is a lack of donating moieties (besides the disordered and partially-occupied water molecules of crystallization). This leads to a general weak supramolecular network which also accounts for the various structural disorder features found in the crystal structure (ESI for additional technical details).

Further synthetic work was focused on the elaboration of 1,4-disubstituted 1,2,3-triazole-*O*-acridinedione/*O*-xanthenedione and 3,5-disubstituted 1,2-isoxazole-*O*-acridinedione/*O*-xanthenedione hybrid compounds, and this time, we start with the alkylation of commercially available hydroxybenzaldehydes **13a-d** using propargyl bromide in the presence of K₂CO₃ to give the corresponding propargyloxybenzaldehydes **14a-d**, bearing an alkynyl group required for click chemistry (Scheme 4). Compounds **14a-d** are then subjected to click chemistry, as previously reported by employing arylazides **8a,b** in the presence of CuSO₄·5H₂O and sodium ascorbate as the catalytic system in dichloromethane:H₂O (2:1, v/v) at room temperature for 12 h. This provides 1,4-disubstituted 1,2,3-triazolealdehydes **15a-e** in good yields (55-88%).²⁷

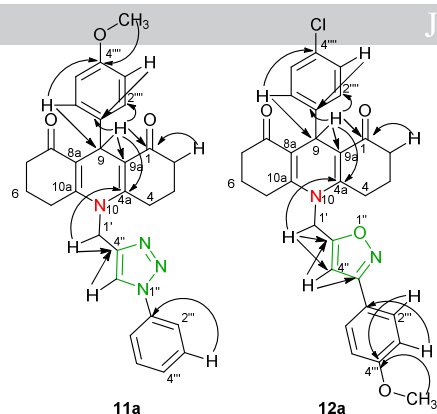


Figure 2. Main HMBC correlation observed for *N*-1,2,3-triazole-dioxodecahydroacridine **11a** and *N*-1,2-isoxazole-dioxodecahydro-acridine **12a**.

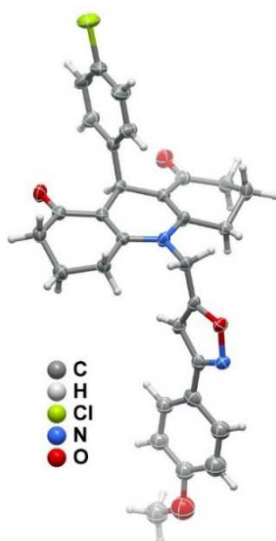
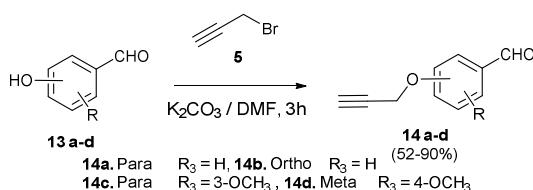


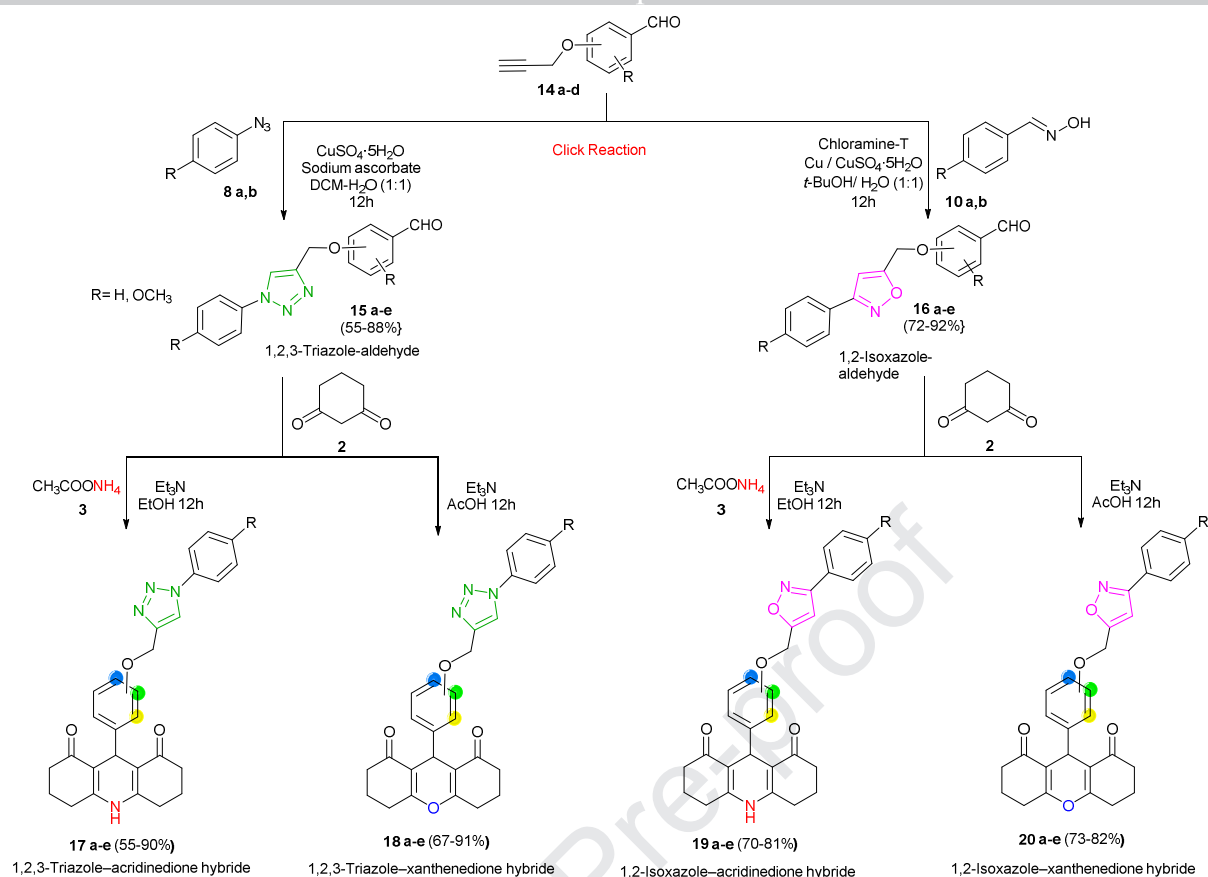
Figure 3. Schematic representation of the molecular units present in the crystal structure of compound **12a**·0.8CH₂Cl₂·0.4H₂O. Non-hydrogen atoms are represented as thermal ellipsoids drawn at the 50% probability level (except for those which were refined isotropically – see ESI for additional technical details), and hydrogen atoms as small spheres with arbitrary radii.



Scheme 4. Synthesis of propargyloxybenzaldehydes **14a-c**.

In the same fashion as mentioned above, we prepare 1,2-isoxazolealdehydes **16a-e** by click reaction of aryloximes **10a,b** with propargyloxyaldehydes **14a-d** in the presence of chloramine-T, CuSO₄ and Cu powder as a catalyst, being the desired 1,2-isoxazolealdehydes **16a-e** also obtained in good yields (72-92%). The ending step of our synthetic strategy aims at the production of 1,2,3-triazole-*O*-acridinediones **17a-e** and 1,2-isoxazole-*O*-acridinediones **19a-e** hybrids by a Hantzsch reaction. We therefore performed the one-pot three-component reaction between two molecules of 1,3-cyclohexanedione, the corresponding triazole-aldehydes **15a-e** or isoxazole-aldehydes **16a-e** and ammonium acetate using triethylamine as a catalyst in ethanol.

The target heterocyclic hybrids **17a-e** and **19a-e** were isolated in good to excellent yields (55-90%) (Scheme 5).²⁶ In addition, we have investigated another MCR route for the synthesis of 1,2,3-triazole-*O*-xanthenediones **18a-e** and 1,2-isoxazole-*O*-xanthenediones **20a-e** hybrids by using two molecules of 1,3-cyclohexanedione and the corresponding triazole-aldehydes **15a-e** or isoxazole-aldehydes **16a-e** with triethylamine as catalyst in acetic acid to afford the desired compounds **18a-e** and **20a-e** in very good yields (67-91%)²⁸ (Scheme 5).



Scheme 5. Synthesis of *O*-1,2,3-triazole-acridinediones **17a-e**, *O*-1,2,3-triazole-xanthenediones **18a-e**, *O*-1,2-isoxazole-acridinediones **19a-e** and *O*-1,2-isoxazole-xanthenediones **20a-e**.

The examination of the NMR spectra of our novel heterocyclic hybrids 1,2,3-triazole-*O*-acridinediones/*O*-xanthenediones **17a-e**, **18a-e** and 1,2-isoxazole-*O*-acridinediones/*O*-xanthenediones **19a-e**, **20a-e** suggests that most of the pure products are obtained in a regioselective manner affording 1,4-disubstituted 1,2,3-triazoles and 3,5-disubstituted isoxazoles linked to acridinediones or xanthenediones. From the ^1H NMR and 2D-HSQC spectra of these compounds, we could distinguish two characteristic groups 9-*CH* (δ_{H} 4.54-5.15 ppm, δ_{C} 30.4-32.0 ppm) and 1''-*CH*₂ (δ_{H} 5.14-5.26 ppm, δ_{C} 60.5-62.0 ppm), being considered as the linking bridges between the acridine or xanthene skeleton and the triazole or isoxazole heterocycles. The triazole and isoxazole protons H-5''' and H-4''' appear as a singlet at δ_{H} 8.89-8.90 and 7.12-7.16 ppm, respectively. The cyclohexanone parts can be characterized through their aliphatic protons at δ_{H} 1.78-1.90 ppm for H-3/6, 2.11-2.28 ppm for H-2/7 and 2.43-2.53 ppm for H-4/5 (case of compound **17a**).

From the ^{13}C NMR and 2D-HSQC spectra, all the protonated carbon have been successfully assigned, mainly those of the cyclohexanone structure δ_{C} 21.3 ppm for C-3/6, 26.8 ppm for C-4/5 and 37.2 for C-2/7 (case of compound **17a**). However, it was possible to differentiate between these aliphatic carbons only by interpreting the 2D-HMBC spectrum of compound **17a**, where we find 10-NH (δ_{H} 9.37 ppm) establishing remarkable $J^3_{\text{H/C}}$ HMBC correlation with the aliphatic carbon C-4/5. Other interesting HMBC connectivities have been observed for the 10-NH with the quaternary carbons of the cyclic acridine skeleton, where we could attribute C8a/9a to δ_{C} 113.1 ppm via $J^3_{\text{H/C}}$ correlation of 10-NH and C-4a/10a to δ_{C} 151.5 ppm via $J^2_{\text{H/C}}$ with this same proton. It was also possible to discover a rare $J^4_{\text{H/C}}$ connection of 10-NH with the carbonyl C-1 (δ_{C} 195.2 ppm),

which help to characterize the hybrid structures **17-20** (Figure 4, ESI for NMR spectra).

To support our regioselective preparation of the reported heterocyclic hybrids, we crystallised selected compounds to be investigated by single-crystal X-ray diffraction. We isolated good crystals of the *O*-isoxazole-acridine hybrid **19b** from an ethanolic solution by slow evaporation at *ca.* 6 °C. The crystal structure was solved and refined in the centrosymmetric monoclinic $P2_1/n$ space group, with the asymmetric unit being composed of a whole molecular unit of **19b** and a partially-occupied water molecule of crystallisation (refined as 75%, Figure 5). Though the molecular unit is rich acceptor atoms capable of engaging in strong and directional hydrogen bonding interactions, there is only one donor group capable of such (besides the partially-occupied water molecule of crystallization): the -NH moiety of the dioxodecahydroacridine. This moiety is indeed engaged in an unique bifurcated N-H...O interaction with the oxygen atoms of a neighboring molecular unit [$d_{\text{N}\dots\text{O}}$ ranging from 2.892(4) to 3.156(3) Å; $\angle(\text{NHO})$ interaction angles in the 115(3)-178(3)° range], forming a $\text{C}^1_1(10)$ graph set motif.²⁹

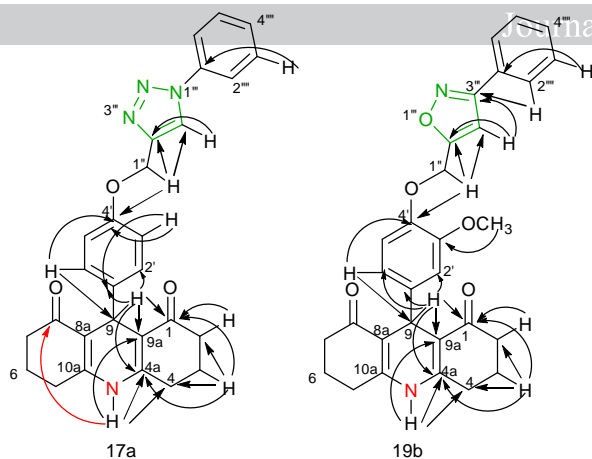


Figure 4. Main HMBC correlations of *N*-1,2,3-triazole-dioxodecahydroacridine **17a** and *N*-1,2-isoxazole-dioxodecahydroacridine **19b**.

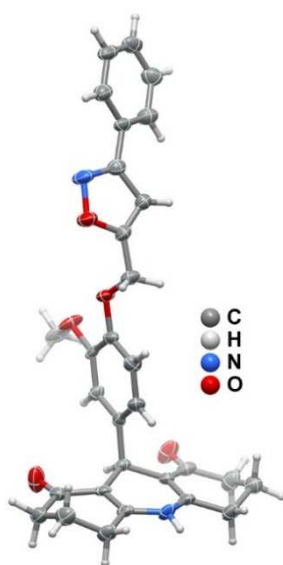


Figure 5. Schematic representation of the molecular unit present in the crystal structure of compound **19b**·0.75H₂O. Non-hydrogen atoms are represented as thermal ellipsoids drawn at the 70% probability level (except for those associated with the disordered methyl group – see the ESI for additional technical details), and hydrogen atoms as small spheres with arbitrary radii.

2.2. *In vitro* evaluation of cytotoxic effects

The cytotoxicity of *N*-1,2,3-triazole-dioxodecahydroacridines **11a-e**, *N*-1,2-isoxazole-dioxodecahydroacridines **12a**, *O*-1,2,3-triazole-acridinediones **17c-d**, *O*-1,2,3-triazole-xanthenediones **18a-e**, *O*-1,2-isoxazole-acridinediones **19b**, **19e** and *O*-1,2-isoxazole-xanthenediones **20a-b**, **20e** have been studied in two human breast cancer cell lines (MDA-MB-231, T47-D) and one prostate cancer cell line (PC3) after 72 h of exposure using the prestoblu method.³⁰ Compounds have been selected upon their optimized solubility in DMSO, hence we started the biological screening by using a 10 nM to 100 μ M concentrations curve with a dilution factor of 10 (doxorubicin is employed as a positive control). Most of the selected compounds displayed less than 60% of inhibitory effects on the tested cancer cell lines at 100 μ M (Figure 6). In prostate cancer cells (PC3), compounds **11c**, **19e** and **20a**

have no considerable effect, while 10% of inhibitory could be observed for compounds **11d**, **17c**, **17d**, **18e** and **20b**. In the other side, compounds **17d**, **20a**, **20b** and **20e** are less active on the breast cancer (T47-D and MDA-MB-231). The most active compounds **11e**, **12a**, **18a-d** exhibited total or near-total cytotoxicity at 100 μ M concentrations, but no effects were observed at concentrations lower than 10 μ M. Therefore, the 10-100 μ M concentration range was expanded to cover values every 0.25 unit to allow calculation of the IC₅₀ values as shown in Table 1.

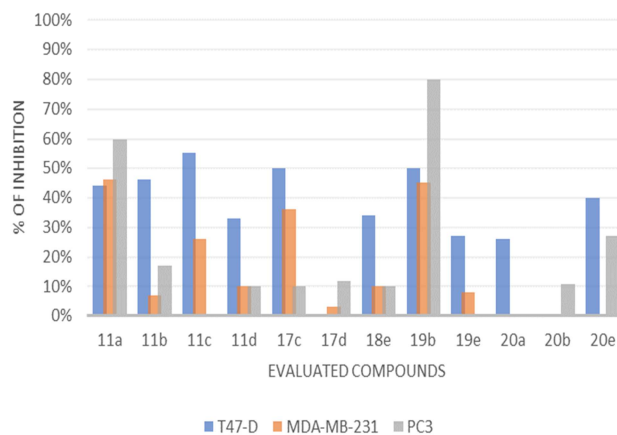


Figure 6. Representative graphic of *in vitro* cytotoxicity assessment of compounds **11a-d**, **17c-d**, **18e**, **19b**, **19e**, **20a-b** and **20e** against breast cancer (T47-D and MDA-MB-231) and prostate cancer (PC3) cell lines at concentration of 100 μ M.

The results showed that in metastatic cancer cell lines (MDA-MB-231) compounds **12a**, **18b** and **18c** displayed IC₅₀ value \leq 20 μ M. Compounds **18b-d** exhibited the highest cytotoxic effect against the non-metastatic cell line (T47-D) with IC₅₀ value \leq 20 μ M (Table 1). The *in vitro* antiproliferative activity of *N*-1,2,3-triazole-dioxodecahydroacridines **11a-e** in both cell lines tested are weak, nevertheless their inhibitory effects are more pronounced in the non-metastatic cells (T47-D) than in the metastatic cells (MDA-MB-231 and PC3) (Figure 6). The *N*-1,2-isoxazole-dioxodecahydroacridine **12a** showed similar cytotoxic effect in T47-D cells comparing to compound **11e**. However, compound **12a** exhibited around 6-fold more potency in MDA-MB-231 cell than compound **11e** (Table 1). These results suggested that the introduction of 1,2-isoxazole molecule at the acridine scaffold may lead to an increased cytotoxicity in metastatic cancer cells. Compounds **12b-e** should be evaluated to confirm these results, however due to some difficulties of solubility in DMSO, the experiments were not performed.

The preliminary evaluation of *in vitro* antiproliferative activity of compounds **17c-d**, **18a-e**, **19b**, **19e**, **20a-b** and **20e** showed that the most active hybrids are *O*-1,2,3-triazole-xanthenediones **18a-d**. Among them, compound **18c** without any substituents in the aromatic rings displayed the most effective cytotoxicity on the tested cancer cell lines with IC₅₀ values less than 20 μ M in case of breast cancer (MDA-MB-231 and T47-D) and have recorded the highest cytotoxic effect in PC3 cells, with IC₅₀ value of 10 μ M (Table 1). These results suggest that the *ortho* position of the 1,2,3-triazole motif at the xanthenedione scaffold favours the cytotoxicity in PC3 cancer cells when comparing to compound **18a**, **18b** and **18d** of the same group. In case of *O*-1,2,3-triazole-

acridinedione **17** and *O*-1,2-isoxazole-acridinedione **19**, no significant inhibitory effects were observed in the tested cancer cells at concentrations below 100 μM . At 100 μM compound **19b** is clearly affecting all cancer cell lines compared to **17d** (Figure 6), which may inform that the conjugation and position of the isoxazole moiety at the acridinedione scaffold is in favour of an increased cytotoxicity.

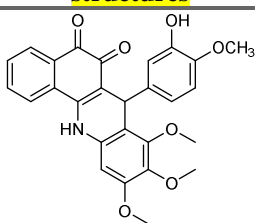
Table 1. In vitro cytotoxicity assessment of compounds **11e**, **12a**, **18a-d** against breast cancer (T47-D and MDA-MB-231) and prostate cancer (PC3) cell lines.

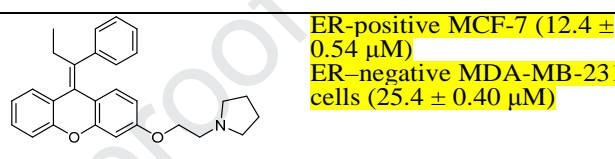
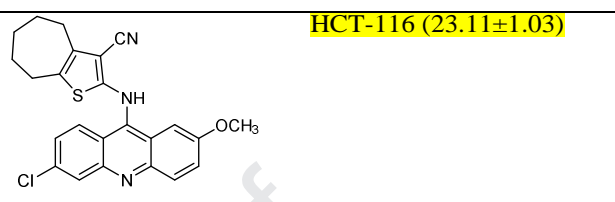
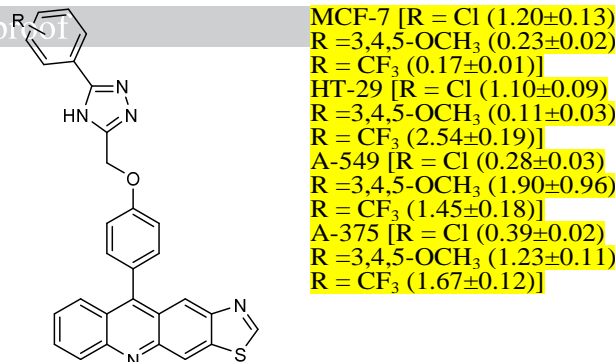
Compound	T47-D IC ₅₀ $\mu\text{M}^{(a)}$	MDA-MB-231 IC ₅₀ $\mu\text{M}^{(a)}$	PC3 IC ₅₀ $\mu\text{M}^{(a)}$
11e	38.05 \pm 4.10	65.35 \pm 3.18	58.19 \pm 3.57
12a	49.02 \pm 1.03	10.78 \pm 0.85	38.65 \pm 4.50
18a	26.70 \pm 0.44	49.45 \pm 1.37	25.86 \pm 0.56
18b	18.40 \pm 3.89	17.69 \pm 1.18	64.58 \pm 2.11
18c	14.50\pm1.59	20.88\pm0.20	10.20\pm0.22
18d	19.40 \pm 1.67	45.31 \pm 0.87	66.84 \pm 1.09
Doxorubicin	0.13 \pm 0.003	1.51 \pm 0.97	0.73 \pm 0.14

[a] IC₅₀ determined by the prestoBlue method after 72h of incubation. Each value is the mean (IC₅₀ \pm SD) of two independent experiments performed in quadruplicate

The cytotoxic activity of reported hybrid compounds sharing acridine/xanthene have resulted in promising antiproliferative activity against a panel of tested cancer cells (Table 2).³¹⁻³⁴ The hybrid acridine-1,2,4-triazole compounds with different substitutions at the *para* position of the phenyl ring exhibited the most potent anticancer activity against four cancer cell lines (MCF-7, HT-29, A-549, A-375) with IC₅₀ values \leq 5 μM .³² Acridine-thiophene hybrids shows selectivity toward HCT-116 cells, whereas no cytotoxicity was observed for other cell lines tested (HeLa, MCF-7, K562, HL-60, HaCat, PBMC).³³ Synthetic xanthene-pyrrolidine was reported to possess comparable behavior to Tamoxifen on ER-positive MCF-7 and ER-negative MDA-MB-231 cells (Table 2).³⁴ Our data screening of cytotoxic effect of 1,2,3-triazole and 1,2-oxazole-acridinediones/xanthenediones heterocyclic hybrids provide essential SAR information and experimental structural models for anticancer drug design.

Table 2. Reported studies of in vitro cytotoxicity assessment of some hybrid compounds against a panel of cancer cell lines.

Organic hybrid structures	Cancer cell lines tested (IC ₅₀ \pm SD μM)
	MCF-7 (16.24 \pm 0.54)
	A2780 (10.43 \pm 1.46)
	HeLa (22.86 \pm 1.45)
	HepG2 (15.07 \pm 1.63)
	DU145 (13.73 \pm 1.26)
	A549(9.01 \pm 0.24)
	PC3 (5.23 \pm 1.37)
	LNCAP (18.54 \pm 2.11)
HUVEC (49.19 \pm 2.3)	



3. Conclusion

In summary, novel series of acridinediones and xanthenediones containing triazole and isoxazole moieties with varied aromatic substitution, all in one hybrid structure, have been synthesized in appreciable yields. The spectral NMR data and single-crystal X-ray have been well exploited to finely characterize the molecular structures with various structural patterns. Different synthetic methodologies have been combined from a one-pot multi-component reaction to 1,3-dipolar cycloaddition and click chemistry in order to achieve a high structural complexity of novel heterocyclic hybrids. The preliminary anticancer screenings on human cancer cell lines demonstrate that the *O*-1,2,3-triazole-xanthenediones hybrids show the best cytotoxic effects. Moreover, *N,O*-isoxazole moiety coupled to the acridinedione scaffold could lead to an increased cytotoxicity. Further antiproliferative studies are required to provide more insights about the combination of heterocyclic pharmacophores in a hybrid molecule and their structure-activity-relationship in cancer therapy.

4. Experimental section

General remarks: Melting points were measured using Kofler bench method. All reactions were followed by TLC (E. Merck Kieselgel 60 F-254), with detection by UV light at 254 nm. ¹H and ¹³C NMR spectra were recorded on a Bruker AC 400 MHZ FTNMR spectrometer using DMSO-d₆ as solvent. Chemical shifts (δ) were reported in parts per million (ppm) relative to tetramethylsilane TMS (δ = 0 ppm) used as an internal reference and coupling constants (*J*) were given in Hz. The following multiplicity abbreviations were used: s, singlet; d, doublet; t, triplet; q, quadruplet; m, multiplet. High-resolution mass spectra (ESI⁺-HRMS) were measured with a microTOF-Q 98 spectrometer. All chemicals and solvents were purchased from commercial sources and used as received.

General procedure for the synthesis of 1,8-dioxodecahydroacridines (4a-e, 17a-e and 19a-e). A

mixture of aldehyde **1a-e** (or **15a-e** / **16a-e**) (1 mmol), 1,3-cyclohexane-dione **2** (2 mmol, 0.224 mg), ammonium acetate **3** (3 mmol, 0.231 mg), triethylamine (2 mmol, 0.202 mg) in ethanol (20 mL) was placed in a 50 mL flask and refluxed under continuous stirring for the appropriate time as monitored by thin-layer chromatography TLC. After completion of the reaction, the solvent was evaporated to give the crude product, which was purified by recrystallization from EtOH to provide the pure product **4a-e** (**17a-e** / **19a-e**) without further purification.

General procedure for the synthesis of *N*-propargylated 1,8-dioxodecahydroacridines and propargyloxybenzaldehydes (**6a-e** and **14a-e**).

A mixture of 1,8-dioxodecahydroacridine **4a-e** (or hydroxybenzaldehyde **13a-e**) derivatives (2 mmol), propargyl bromide **5** (2.2 mmol, 0.262 mg) and K₂CO₃ (4 mmol, 0.552 mg) in *N,N*-dimethylformamide (15 mL) was stirred at room temperature for 3 hours. Water (15 mL) was added to the reaction mixture to be extracted with dichloromethane (3 x 15 mL). The organic layer was dried over anhydrous sodium sulphate, filtered and concentrated. The final residue was recrystallized from ethanol to afford the desired compounds **6a-e** (or **14a-e**).

General synthetic procedure for the aromatic azides 8a,b. The aniline substrate **7a,b** (10 mmol) was dissolved in hydrochloric acid (15 mL) in a round-bottom flask and cooled to 0 °C in an ice bath. Ice cooled sodium nitrite NaNO₂ (12 mmol, 0.830 mg) solution was added into the aniline-acid solution and stirred for 10 min. NaN₃ (12 mmol, 0.780 mg) was then added under stirring for 1 hour. Finally, the solution was extracted with ethyl acetate (3 x 15 mL) and the organic layers were combined and dried over Na₂SO₄. After solvent removal under reduced pressure, the azidobenzene derivatives **8a,b** are afforded.

General procedure for the synthesis of 1,2,3-triazole derivatives via 1,3-dipolar cycloaddition (11a-e and 15a-e). Synthetic phenyl azide derivatives **8a,b** (1 mmol) and 1,8-dioxodecahydroacridine derived alkyne **6a-e** (or propargyloxybenzaldehydes **14a-e**) (1 mmol) were taken in CH₂Cl₂ and H₂O (10 mL, 1:1) system in a 50 mL round bottomed flask. CuSO₄·5H₂O (2.2 mmol, 0.548 mg) and sodium ascorbate (2.8 mmol, 0.554 mg) were added. The reaction mixture was stirred at room temperature for 12 hours under TLC monitoring. After completion of the reaction, the aqueous layer was extracted with CH₂Cl₂ (3 x 15 mL). The combined organic phases were dried over Na₂SO₄ and concentrated under reduced pressure. The obtained crude product was recrystallized from ethanol to afford the pure products **11a-e** (or **15a-e**).

General synthetic procedure for the aldoximes (10a,b). To a methanolic solution of aldehyde **9a,b** (10 mmol), hydroxyl amine hydrochloride (10 mmol, 0.695 mg) was added followed by sodium acetate (10 mmol, 0.770 mg). The mixture was stirred at room temperature. After completion of the reaction as monitored by TLC, water was added to the reaction mixture and then extracted with ethyl acetate (3 x 15 mL). The organic layers were combined and dried over Na₂SO₄. After solvent removal under reduced pressure aldoxime derivatives **10a,b** are afforded.

General procedure for the synthesis of 1,2-isoxazole derivatives via 1,3-dipolar cycloaddition (12a-e and 16a-e). To the appropriate aldoximes **10a,b** (1 mmol) dissolved in 10 mL of *t*-BuOH/H₂O (1:1), chloramine-T trihydrate (2

mmol, 0.455 mg) was gradually added over 3 minutes followed by CuSO₄·5H₂O (1 mmol, 0.250 mg) and copper powder (2 mmol, 0.128 mg). To the aforementioned solution, the appropriate 1,8-dioxodecahydroacridine derived alkyne **6a-e** (or propargyloxybenzaldehydes **14a-e**) (1 mmol) was added and the reaction mixture was stirred for 12 hours at room temperature. Water (10 mL) was added to the reaction mixture and directly extracted with dichloromethane (3 x 15 mL). The organic layer was dried over anhydrous sodium sulfate, filtered, concentrated and then recrystallized from ethanol to give the required isoxazoles **12a-e** (or **16a-e**).

General procedure for the synthesis of 1,8-dioxooctahydroxanthenes 18a-e and 20a-e. A mixture of aldehyde **15a-e** (or **16a-e**) (0.3 mmol), 1,3-cyclohexanedione **2** (0.6 mmol, 0.067 mg) and triethylamine (0.6 mmol, 0.061 mg) as catalyst in 10 mL of acetic acid was allowed to stir at reflux for the appropriate time. After completion of the reaction under TLC monitoring, the solvent was evaporated under vacuum and the solid product obtained was washed with ethanol and then water. The products were purified by recrystallization from ethanol to give the desired compounds **18a-e** (**20a-e**).

9-(4-Methoxyphenyl)-10-[(1-phenyl-1*H*-1,2,3-triazol-4-yl)methyl]-3,4,6,7,9,10-hexahydroacridine-1,8(2*H*,5*H*)-dione (11a): C₂₉H₂₈N₄O₃; MW = 480.56 g/mol; 0.344 g (69.5%); yellow solid; mp 258-260 °C. ¹H NMR (400 MHz, DMSO-*d*₆) δ : 1.85-1.98 (2m, 4H, H-3/6, eq:ax), 2.21-2.28 (m, 4H, H-2/7), 2.64-3.08 (2m, 4H, H-4/5, eq:ax), 3.57 (s, 3H, 4''-OCH₃), 5.02 (s, 1H, H-9), 5.18 (s, 2H, H-1'), 6.58 (d, *J* = 8.7 Hz, 2H, H-3'''/5'''), 6.91 (d, *J* = 8.7 Hz, 2H, H-2'''/6'''), 7.40-7.55 (m, 1H, H-4'''), 7.56-7.70 (m, 2H, H-3'''/5'''), 7.83-7.99 (m, 2H, H-2'''/6'''), 8.75 (s, 1H, H-5'') ppm. ¹³C NMR (100 MHz, DMSO-*d*₆) δ : 21.5 (C-3/6), 26.7 (C-4/5), 30.1 (C-9), 36.4 (C-2/7), 41.1 (C-1'), 55.4 (4''-OCH₃), 113.5 (C-3'''/5'''), 116.0 (C-8a/9a), 120.4 (C-2'''/6'''), 121.8 (C-5''), 128.7 (C-2'''/6'''), 129.4 (C-4'''), 130.3 (C-3'''/5'''), 136.9 (C-1'''), 139.1 (C-1'''), 145.2 (C-4''), 153.9 (C-4a/10a), 157.6 (C-4'''), 195.8 (C-1/8, C=O) ppm. HRMS (ESI⁺): *m/z* calcd for [C₂₉H₂₈N₄O₃+H]⁺: 481.2161; found: 481.2234.

9-(4-Chlorophenyl)-10-[[3-(4-methoxyphenyl)isoxazol-5-yl]methyl]-3,4,6,7,9,10-hexahydroacridine-1,8(2*H*,5*H*)-dione (12a): C₃₀H₂₇ClN₂O₄; MW = 515.01 g/mol; 0.331 g (64.3%); white solid; mp 142-144°C. ¹H NMR (400 MHz, DMSO-*d*₆) δ : 1.84-1.98 (2m, 4H, H-3/6, eq:ax), 2.18-2.31 (m, 4H, H-2/7), 2.57-2.96 (2m, 4H, H-4/5, eq:ax), 3.83 (s, 3H, 4''-OCH₃), 5.10 (s, 1H, H-9), 5.29 (s, 2H, H-1'), 6.89 (s, 1H, H-4''), 7.03-7.14 (m, 4H, H-3'''/5''', H-2'''/6'''), 7.17 (d, *J* = 8.5, 2H, H-3'''/5'''), 7.78 (d, *J* = 8.8, 1H, H-2'''/6''') ppm. ¹³C NMR (100 MHz, DMSO-*d*₆) δ(ppm): 21.4 (C-3/6), 26.3 (C-4/5), 30.6 (C-9), 36.5 (C-2/7), 42.0 (C-1'), 55.8 (4''-OCH₃), 101.0 (C-4''), 115.1 (C-3'''/5'''), 115.2 (C-8a/9a), 120.9 (C-1'''), 128.2 (C-3'''/5'''), 128.6 (C-2'''/6'''), 129.5 (C-2'''/6'''), 130.9 (C-4'''), 145.4 (C-1'''), 154.2 (C-4a/10a), 161.2 (C-4'''), 162.10 (C-3'''), 169.4 (C-5''), 195.7 (C-1/8, C=O) ppm. HRMS (ESI⁺): *m/z* calcd for [C₃₀H₂₇ClN₂O₄+H]⁺: 515.1659; found: 515.1732.

9-{4-[(1-Phenyl-1*H*-1,2,3-triazol-4-yl)methoxy]phenyl}-3,4,6,7,9,10-hexahydroacridine-1,8(2*H*,5*H*)-dione (17a): C₂₈H₂₆N₄O₃; MW = 466.54 g/mol; 0.409 g (87.6%); white solid; mp > 260 °C. ¹H NMR (400 MHz, DMSO-*d*₆) δ 1.78-1.90 (2m, 4H, H-3/6, eq:ax), 2.11-2.28 (m, 4H, H-2/7), 2.43-2.53 (m, 4H, H-4/5, eq:ax), 4.86 (s, 1H, H-9), 5.14 (s,

2H, H-1''), 6.86 (d, $J = 8.7$, 2H, H-3'/5'), 7.08 (d, $J = 8.7$, 2H, H-2'/6'), 7.45-7.53 (m, 1H, H-4'''), 7.55-7.64 (m, 2H, H-3'''/5'''), 7.86-7.95 (m, 2H, H-2'''/6'''), 8.89 (s, 1H, H-5'''), 9.37 (s, 1H, 10-NH) ppm. ^{13}C NMR (100 MHz, DMSO- d_6) δ : 21.3 (C-3/6), 26.8 (C-4/5), 31.6 (C-9), 37.2 (C-2/7), 61.5 (C-1''), 113.1 (C-8a/9a), 114.4 (C-3'), 120.6 (C-2'''/6'''), 123.3 (C-5'''), 128.9 (C-2'), 129.2 (C-4'''), 130.3 (C-3'''/5'''), 137.0 (C-1'''), 140.6 (C-1'), 144.6 (C-4'''), 151.5 (C-4a/10a), 156.4 (C-4'), 195.2 (C-1/8, C=O) ppm. HRMS (ESI⁺): m/z calcd for $[\text{C}_{28}\text{H}_{26}\text{N}_4\text{O}_3+\text{H}]^+$: 467.2005; found: 467.2078.

9-[4-[(1-(4-Methoxyphenyl)-1H-1,2,3-triazol-4-yl)methoxy]phenyl]-3,4,5,6,7,9-hexahydro-1H-xanthene-1,8(2H)-dione (18b): $\text{C}_{29}\text{H}_{27}\text{N}_3\text{O}_5$; MW = 497.55 g/mol; 0.126 g (84.4%); brown solid; mp 178-182 °C. ^1H NMR (400 MHz, DMSO- d_6) δ 1.74-2.02 (2m, 4H, H-3/6, eq:ax), 2.15-2.37 (m, 4H, H-2/7), 2.53-2.74 (m, 4H, H-4/5, eq:ax), 3.83 (s, 3H, 4'''-OCH₃), 4.54 (s, 1H, H-9), 5.14 (s, 2H, H-1''), 6.81-6.98 (m, 2H, H-3'), 7.12 (m, 4H, H-2'/3'''), 7.69-7.89 (m, 2H, H-2'''), 8.79 (s, 1H, H-5''') ppm. ^{13}C NMR (100 MHz, DMSO) δ 20.4 (C-3/6), 26.9 (C-4/5), 30.4 (C-9), 36.9 (C-2/7), 56.0 (4'''-OCH₃), 61.5 (C-1''), 114.6, (C-3'), 115.3, B (C-3'''), 116.2 (C-8a, C-9a), 122.3 (C-2'''), 123.2 (C-5'''), 129.5, (C-2'), 130.5, (C-1'''), 137.7 (C-1'), 144.2, (C-4'''), 156.9 (C-4'), 159.8 (4'''-OCH₃), 165.1 (C-4a, C-10a), 196.8 (C-1/8, C=O) ppm. HRMS (ESI⁺): m/z calcd for $[\text{C}_{29}\text{H}_{27}\text{N}_3\text{O}_5+\text{H}]^+$: 498.1951; found: 498.2023.

9-(3-Methoxy-4-[(3-phenylisoxazol-5-yl)methoxy]phenyl)-3,4,6,7,9,10-hexahydroacridine-1,8(2H,5H)-dione (19b): $\text{C}_{30}\text{H}_{28}\text{N}_2\text{O}_5$; MW = 496.56 g/mol; 0.388g (78.1%); white solid; mp 232-234 °C. ^1H NMR (400 MHz, DMSO- d_6) δ : 1.69-1.86 (2m, 4H, H-3/6, eq:ax), 2.15-2.28 (m, 4H, H-2/7), 2.43-2.58 (m, 4H, H-4/5, eq:ax), 3.71 (s, 3H, 3'-OCH₃), 4.89 (s, 1H, H-9), 5.19 (s, 2H, H-1''), 6.61 (dd, $J = 8.3$, 1.9, 1H, H-6'), 6.85 (d, $J = 1.9$, 1H, H-2'), 6.89 (d, $J = 8.3$, 1H, H-5'), 7.12 (s, 1H, H-4'''), 7.52 (m, 3H, H-4''', H-3'''/5'''), 7.88 (m, 2H, H-2'''/6'''), 9.39 (s, 1H, 10-NH) ppm. ^{13}C NMR (100 MHz, DMSO- d_6) δ (ppm): 21.4 (C-3/6), 26.8 (C-4/5), 31.7 (C-9), 37.2 (C-2/7), 55.9 (3'-OCH₃), 62.0 (C-1''), 102.7 (C-4'''), 112.8 (C-8a/9a), 112.9 (C-2'), 114.7 (C-5'), 119.4 (C-6'), 127.1 (C-2'''/6'''), 128.8 (C-1'''), 129.6 (C-3'''/5'''), 130.8 (C-4'''), 142.1 (C-1'), 145.4 (C-4'), 149.0 (C-3'), 151.7 (C-4a/C-10a), 162.4 (C-3'''), 169.4 (C-5'''), 195.4 (C-1/8, C=O) ppm. HRMS (ESI⁺): m/z calcd for $[\text{C}_{30}\text{H}_{28}\text{N}_2\text{O}_5+\text{H}]^+$: 497.1998; found: 497.2071.

9-[4-[(3-phenylisoxazol-5-yl)methoxy]phenyl]-3,4,5,6,7,9-hexahydro-1H-xanthene-1,8(2H)-dione (20a): $\text{C}_{29}\text{H}_{25}\text{NO}_5$; MW = 467.52 g/mol; 0.106g (75.5%); white solid; mp 238-240 °C ^1H NMR (400 MHz, DMSO- d_6) δ : 1.74-2.01 (2m, 4H, H-3/6, eq:ax), 2.19-2.35 (m, 4H, H-2/7), 2.57 - 2.73 (m, 4H, H-4/5, eq:ax), 4.51-4.57 (s, 1H, H-9), 5.14-5.37 (s, 2H, H-1''), 6.85-6.97 (d, $J = 8.2$ Hz, 2H, H-3'), 7.06-7.15 (d, $J = 8.4$ Hz, 2H, H-2'), 7.15-7.24 (s, 1H, H-4'''), 7.41-7.63 (q, $J = 3.2$, 2.3 Hz, 3H, H-3'''/4'''), 7.78-7.96 (m, 2H, H-2''') ppm. ^{13}C NMR (100 MHz, DMSO) δ 20.2 (C-3/6), 26.9 (C-4/5), 30.4 (C-9), 36.8 (C-2/7), 60.9 (C-1''), 102.6 (C-4'''), 114.6 (C-3'), 116.1 (C-8a/9a), 127.1 (C-2'''), 128.8 (C-1'''), 129.5 (C-3'''), 129.6 (C-2'), 130.8 (C-4'''), 138.2 (C-1'), 156.4 (C-4'), 162.4 (C-3'''), 165.1 (C-4a/10a), 169.2 (C-5'''), 196.8 (C-1/8, C=O). HRMS (ESI⁺): m/z calcd for $[\text{C}_{29}\text{H}_{25}\text{NO}_5+\text{H}]^+$: 468.1811; found: 468.1688.

Biological screening

Cell culture: MDA-MB-231 metastatic breast cancer cell line was grown in DMEM culture medium supplemented with 10% fetal bovine serum (FBS) (Gibco™ by Life Technology) and 1% penicillin/streptomycin solution (PEST; Gibco™). T47-D non-metastatic luminal breast cancer and PC3 metastatic prostate cancer cell lines were grown in RPMI culture medium supplemented with 10% FBS and 1% PEST. Cell cultures were maintained at 37 °C in a 5% CO₂ humidified atmosphere.

Reagent and tested compounds: Compounds were dissolved in 100% DMSO to obtain a stock concentration of 100 mM. Thereafter, serial dilutions were prepared in growth medium. Maximum DMSO concentration applied to the cells was 0.1% v/v to avoid toxic effects associated to higher concentrations of this solvent.

Cell viability assay: Serial dilutions ranged from 10nM to 100 μM are prepared to cover a wide scale for generation of dose-response curves. In all experiments, the solvent DMSO (0.1% v/v) alone was used as negative control. Ten thousand cells/wells were seeded in 96-well plates and allowed to adhere for 24 h. Cells were then exposed to the test compounds diluted in culture medium for 48 hours (200 μL), after this time 100 μL of the culture medium was replaced by test solution for additional 24 h. Thereafter, cell viability was assessed using 100 μL /well of the rezasurin-based prestoBlue™ reagent (Life Technologies) according to the manufacturer's instructions. Values considered after 3 h of incubation were within the linear range of the reading. The IC₅₀ values from at least three independent experiments were calculated using GraphPad Prism software (version 6.00), using the log (inhibitor) vs. response (variable slope-four parameters) function.

Acknowledgments

Thanks are due to FCT/MEC for the financial support for the project PT-DZ/0005, of the QOPNA research Unit (FCT UID/QUI/00062/2019) and CICECO – Aveiro Institute of Materials (FCT Ref. UID/CTM/50011/2019) through national funds and, where applicable, co-financed by the FEDER, within the PT2020 Partnership Agreement, and to the Portuguese NMR Network. We would like to thank the General Directorate for Scientific Research and Technological Development – DGRSDT of Algeria and Agence Thématique de Recherche en Sciences et Technologie ATRST for approving the co-financed bilateral project PT-DZ/0005. We further wish to thank CICECO for funding the purchase of the single-crystal X-ray diffractometer. The authors are thankful to Pr. Farid Messelmi the Dean of Faculty of Exact Sciences and informatics in Djelfa University, for providing necessary laboratory facilities.

References and notes

- (a) V. Dave, K. Tak, A. Sohga, A. Gupta, V. Sadhu, K. R. Reddy, *J. Microbiol. Methods* **2019**, *160*, 130-142. (b) V. Dave, A. Gupta, P. Singh, C. Gupta, V. Sadhu, K. R. Reddy, *Nano-Structures and Nano-Objects* **2019**, *18*, 100288. (c) S. Gulla, D. Lomada, V. V. S. S. Srikanth, M. V. Shankar, K. R. Reddy, Sarvesh Soni, M. C. Reddy, *Methods in Microbiology* **2019**, *46*, 255-293. (d) C. Praveen Kumar, T. S. Reddy, P. S. Mainkar, V. Bansal, R. Shukla, S. Chandrasekhar and H. M. Hügel, *Eur. J. Med. Chem.*, **2016**, *108*, 674-686.
- (a) P. Wark, *Respiratory Medicine*, **2004**, *98*, 915-923. (b) Y. Hu, C. Li, X. Wang, Y. Yang, H. Zhu, *Chem. Rev.*, **2014**, *114*, 5572-

5610. (c) S. A. Steiger, C. Li, D. S. Backos, P. Reigan, N.R. Natale, *Bioorg. Med. Chem.*, **2017**, *12*, 3223-3234.
3. (a) D. Dheer, V. Singh, R. Shankar, *Bioorg. Chem.*, **2017**, *71*, 30-54. (b) Z.Najafi, M. Mahdavi, M. Saedi, E. K. Razkenari, N. Edraki, M. Sharifzadeh, M. Khanavi, T. Akbarzadeh, *Bioorg. Chem.*, **2019**, *83*, 303-316. (c) P. De Andrade, S. P. Mantoani, P. Sérgio, G. Nunes, C. R. Magadán, C. Pérez, D. J. Xavier, E. Tiemi, S. Hojo, N. E. Campillo, A. Martínez and I. Carvalho, *Bioorg. Med. Chem.*, **2019**, *27*, 931-943.
 4. C. D. Hein, X.-M. Liu, D. Wang, *Pharm. Res.*, **2008**, *25*, 2216-2230.
 5. S. K. Mamidyala and M. G. Finn, *Chem. Soc. Rev.*, **2010**, *39*, 1252.
 6. S. Kantheti, R. Narayan, K. V. S. N. Raju, *RSC Adv.*, **2015**, *5*, 3687-3708.
 7. K. Chiotos, N. Vendetti, T. E. Zaoutis, J. Baddley, L. Ostrosky-Zeichner, P. Pappas, B. T. Fisher, *J. Antimicrob. Chemother.*, **2016**, *71*, 3536-3539.
 8. A. Singh, S. T. Saha, S. Perumal, M. Kaur, V. Kumar, *ACS Omega*, **2018**, *3*, 1263-1268.
 9. L. D. Bailey, R. V. Kalyana Sundaram, H. Li, C. Duffy, R. Aneja, A. Rosemary Bastian, A. P. Holmes, K. Kamanna, A. A. Rashad, I. Chaiken, *ACS Chem. Biol.*, **2015**, *10*, 2861-2873.
 10. K. Lal, P. Yadav, A. Kumar, A. Kumar, A. K. Paul, *Bioorg. Chem.*, **2018**, *77*, 236-244.
 11. H. M. Faidallah, S. S. Panda, J. C. Serrano, A. S. Girgis, K. A. Khan, K. A. Alamry, T. Therathanakorn, M. J. Meyers, F. M. Sverdrup, C. S. Eickhoff, S. G. Getchell, A. R. Katritzky, *Bioorg. Med. Chem.*, **2016**, *24*, 3527-3539.
 12. A. Anand, M. V. Kulkarni, S. D. Joshi, S. R. Dixit, *Bioorg. Med. Chem. Lett.*, **2016**, *26*, 4709-4713.
 13. F. Harris, L. Pierpoint, *Med Res Rev*, **2012**, *29*, 1292-1327.
 14. D. A. Talan, W. R. Mower, A. Krishnadasan, F. M. Abrahamian, F. Lovecchio, D. J. Karras, M. T. Steele, R. E. Rothman, R. Hoagland, G. J. Moran, *N. Engl. J. Med.*, **2016**, *374*, 823-832.
 15. (a) V. D. da Silva, B. M. de Faria, E. Colombo, L. Ascari, G. P. A. Freitas, L. S. Flores, Y. Cordeiro, L. Romão, C. D. Buarque, *Bioorg. Chem.*, **2019**, *83*, 87-97. (b) K. S. Raju, S. AnkiReddy, G. Sabitha, V. S. Krishna, D. Sriram, K. B. Reddy, S. R. Sagurthi, *Bioorg. Med. Chem. Lett.*, **2019**, *29*, 284-290. (c) S. Burra, V. Voora, Ch. P. Rao, P. V. Kumar, R. K. Kancha, G. L. D. Krupadanam, *Bioorg. Med. Chem. Lett.*, **2017**, *27*, 4314-4318. (d) N. G. Khaligh, T. Mihankhah, M. R. Johan, *J. Mol. Liq.*, **2019**, *277*, 794-804.
 16. (a) F. Bossert, W. Vater, *Med. Res. Rev.*, **1989**, *9*, 291-324. (b) S. M. Derayea, D. M. Nagy, *Rev. Anal. Chem.*, **2018**, *37*, 1-14. (c) A. Kumar, K. M. Rao, S. S. Han, *Carbohydr. Polym.*, **2018**, *180*, 128-144. (d) L. Hellen, S. Matos, F. T. Masson, L. A. Simeoni, M. Homem-de-mello, *Eur. J. Med. Chem.*, **2018**, *143*, 1779-1789.
 17. D. J. Triggie, *Cell Mol. Neurobiol.*, **2003**, *23*, 293-303.
 18. S. Sivapalarajah, M. Krishnakumar, H. Bickerstaffe, Y. Y. Chan, J. Clarkson, A. Hampden-Martin, A. Mirza, M. Tanti, A. Marson, M. Pirmohamed, N. Mirza, *Epilepsia*, **2018**, *59*, 492-501.
 19. A. G. Banerjee, L. P. Kothapalli, P. A. Sharma, A. B. Thomas, R. K. Nanda, S. K. Shrivastava and V. V. Khatanglekar, *Arab. J. Chem.*, **2016**, *9*, S480-S489.
 20. K. R. M. Naidu, B. S. Krishna, M. A. Kumar, P. Arulselvan, S. I. Khalivulla, O. Lasekan, *Molecules*, **2012**, *17*, 7543-7555.
 21. S. Naseem, M. Khalid, M. N. Tahir, M. A. Halim, A. A. C. Braga, M. M. Naseer, Z. Shafiq, *J. Mol. Struct.*, **2017**, *1143*, 235-244.
 22. J. R. Kim, S. Michielsen, *J. Photochem. Photobiol.*, **2015**, *150*, 50-59.
 23. G. Harichandran, S. D. Amalraj, P. Shanmugam, *J. Mol. Catal. A Chem.*, **2014**, *392*, 31-38.
 24. P. Tiposoth, S. Khamsakhon, N. Ketsub, T. Pongtharankul, I. Takashima, A. Ojida, I. Hamachi, J. Wongkongkatap, *Sensor Actuat B-Chem.*, **2015**, *209*, 606-612.
 25. L. Malfatti, K. Suzuki, A. Erker, Y. Jang, P. Innocenzi, *J. Photochem. Photobiol.*, **2018**, *357*, 30-35.
 26. A. Djemoui, M. R. Ouahrani, A. Naouri, L. Souli, S. Rahmani, M. B. Lahrech, *Heterocycl. Lett.*, **2018**, *8*, 455-467.
 27. X. Creary, A. Anderson, C. Brophy, F. Crowell, Z. Funk, *J. Org. Chem.*, **2012**, *77*, 8756-8761.
 28. A. Naouri, A. Djemoui, M. B. Lahrech, S. Rahmani and M. R. Ouahrani, *Heterocycl. Lett.*, **2017**, *7*, 589-597.
 29. J. Grell, J. Bernstein, G. Tinhofer, *Acta Cryst. B*, **1999**, *55*, 1030-1043.
 30. L. Saidi, D. H. A. Rocha, O. Talhi, Y. Bentarzi, B.-Nedjar-Kolli, K. Bachari, F. A. A. Paz, L. A. Helguero, A. M. S. Silva, *Chem. Med. Chem.*, **2019**, *14*, 1041-1048.
 31. F. S. Behbahani, J. Tabeshpour, S. Mirzaei, S. Golmakaniyoon, Z. Tayarani-Najaran, A. Ghasemi, R. Ghodsi, *Arch. Pharm. Chem. Life Sci.* **2019**, 352:e1800307.
 32. S. Mahantia, S. Sunkara, R. Bhavanib, *Synth. Comm.* **2019**, *49*, 1729-1740.
 33. T. Lisboa, D. Silva, S. Duarte, R. Ferreira, C. Andrade, A. L. Lopes, J. Ribeiro, D. Farias, R. Moura, M. Reis, K. Medeiros, H. Magalhães, M. Sobral, *Molecules* **2020**, *25*, 64.
 34. E. Catanzaro, F. Seghettib, C. Calcabrina, A. Rampab, S. Gobbib, P. Sestilic, E. Turrinia, F. Maffea, P. Hreliad, A. Bisib, F. Bellutib, C. Fimognari, *Bioorg. Chem.* **2019**, *86*, 538-549.

Supplementary Material

Supplementary material is available [NMR data and spectra plus crystallographic details].

Highlights:

- 1,2,3-triazole-acridinedione/xanthenedione and 1,2-isoxazole-acridinedione/xanthenedione heterocyclic hybrids have been synthesized via 1,3-dipolar coupling reaction
- 1D, 2D NMR and single-crystal X-ray diffraction analysis confirmed the hybrid structure.
- Anti-proliferative potential in breast and prostate cancer cell lines have been evidenced for the O-1,2,3-triazole-xanthenedione hybrid molecules.

Journal Pre-proof

Declaration of interests

The authors declare that they have no known competing financial interests or personal relationships that could have appeared to influence the work reported in this paper.

Journal Pre-proof